Packing Fraction Analysis for E08-027

Melissa Cummings
The College of William and Mary
melissac@jlab.org

Abstract

The g_2^p experiment aims to study the structure of the proton, but our NH_3 target is not a pure proton target. Events that scatter from unpolarized target material will dilute the e-P scattering asymmetry. To correct for this, a dilution factor correction is applied. The dilution factor represents the ratio of the electron rate from the free, polarizable protons to the total rate from all nucleons in the material. To understand the dilution factor, we must first extract the *packing fraction*, or the proportion of ammonia target material to the liquid helium in which it is immersed. This document will discuss the procedure for extracting the packing fraction along with the resulting values for each target material.

1 Introduction

The packing fraction (p_f) describes the proportion of ammonia target material to the liquid helium in which it is immersed. Ideally, each target cell would be completely full of ammonia, but due to the size and shape of the ammonia beads along with different load sizes, the packing fraction can change for each material sample. To extract the packing fraction, elastic events are analyzed; this allows for good separation of the nitrogen and hydrogen elastic peaks. During the experiment, runs were also taken on a target cell identical to the production cell, but without any ammonia material; these runs are known as "dummy" runs. The dummy runs are useful in understanding the contribution from the helium elastic peak. For this document, the 2.2 GeV, 2.5T, transverse setting will be used as an example to describe the analysis, and the final p_f values will be shown in the results section.

2 g_2^p Target Stick

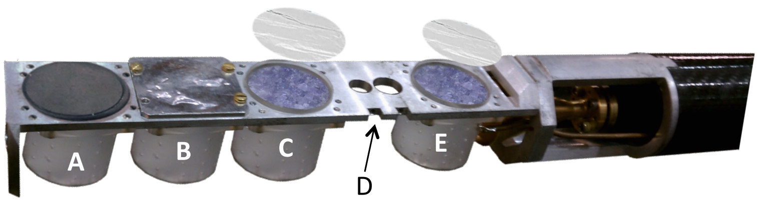

Figure 1: Target stick used for the g_2^p experiment.

The g_2^p target stick is comprised of several different targets, shown in Fig. 1. There are two production target cells (C and E), which are filled with ammonia beads. In addition, a dummy cell (B), which is identical to the production cell but without the ammonia material, and a carbon foil (A) are used for packing fraction and dilution analysis. Finally, there are two empty holes (D), which allow for additional carbon foils to be placed on the target stick, and are also used for centering the beam. The target cell has a radius of 1.361 cm and a length of 2.827 cm. The target stick was inserted into a target nose filled with liquid helium, which was used to cool the target. A diagram of the target setup is seen in Fig. 2.

3 Method

This analysis will utilize data taken at the elastic setting. For the 2.2 GeV, 2.5T setting, there is good separation between the nitrogen and hydrogen elastic peaks. To extract the packing fraction, two types of runs are needed, a production run, and a dummy run. The normalized yield for each run is calculated as:

$$Y = \frac{p_s \cdot N}{Q \cdot LT \cdot \epsilon}, \tag{1}$$

where:

N = number of events
$\mathbf{p_s}$ = prescale factor
Q = total charge for the run
LT = Livetime correction to account for computer deadtime in the system
$\boldsymbol{\epsilon}$ = product of detector efficiencies including scintillator trigger efficiency [4], Cherenkov and lead glass calorimeter detector efficiencies [5] and multitrack efficiency [6].

The yield from a production run can be broken into its constituent parts, as shown in Eq. 2.

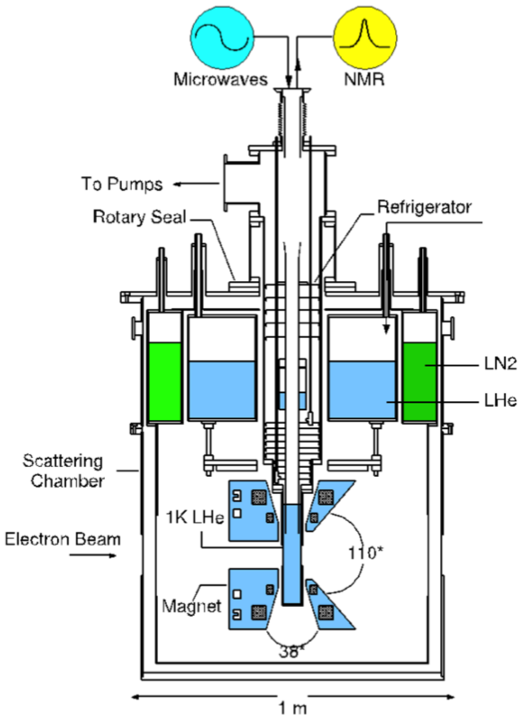

Figure 2: Target setup for the g_2^p experiment.

$$Y_{prod} = Y_{He}^{out} + (1 - p_f)Y_{He}^{full} + p_f Y_{NH_3}^{full}, \tag{2}$$

where Y_x refers to the yield from ammonia (NH_3) and helium (He). The superscript "full" refers to the yield resulting from a target cell full of that material. The superscript "out" refers to the yield from liquid helium inside the target nose, but outside the target cell. The contributions from helium can be obtained by using the yield from a dummy run, Y_{dummy}:

$$Y_{He}^{out} = \left(\frac{l_{tot} - l_{tg}}{l_{tot}}\right) Y_{dummy} \tag{3}$$

$$Y_{He}^{full} = \left(\frac{l_{tg}}{l_{tot}}\right) Y_{dummy}. \tag{4}$$

A simple diagram of the target cell is shown in Fig. 3, which shows the length of the target cell (l_{tg}) and the total length of the target nose (l_{tot}).

Eq. 2 can be manipulated to solve for p_f:

$$p_f = \left(\frac{l_{tot}}{l_{tg}}\right)\left(\frac{Y_{prod}}{Y_{dummy}} - 1\right)\left(\frac{Y_{NH_3}^{full}}{Y_{He}^{full}} - 1\right)^{-1} \tag{5}$$

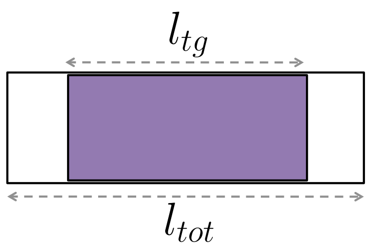

Figure 3: Diagram of the target cell in the target nose. The length of the target cell is given by l_{tg} while the full length of the target nose is given by l_{tot}

From the data, it is not possible to obtain $Y_{NH_3}^{full}$. For this piece of the equation, cross section input from elastic form factor models is used. Although it is possible to extract the quantity Y_{He}^{full}, as shown in Eq. 4, it is advantageous to leave Eq. 5 in this form so that absolute cross sections are not necessary; the acceptance factors will cancel out in the cross section ratio. In terms of the cross section, the yield can be expressed as such:

$$Y_x \sim \sigma_x \cdot \rho_x \tag{6}$$

The cross section input σ_x will be discussed later in this document. The target number density, ρ_x is expressed by Eq. 7:

$$\rho_x = \frac{\rho_{mass} \cdot l_x \cdot N_A}{M_{molar}}, \tag{7}$$

where ρ_{mass}, l_x, and M_{molar} are the mass density, length, and molar mass of the material, respectively and N_A is Avagadro's number. Substituting Eq. 6 into Eq. 5 gives the following expression for the packing fraction:

$$p_f = \left(\frac{l_{tot}}{l_{tg}}\right)\left(\frac{Y_{prod}}{Y_{dummy}} - 1\right)\left(\frac{\sigma_N \frac{\rho_{mass,N}}{M_N} + \sigma_H \frac{\rho_{mass,H}}{M_H}}{\sigma_{He}\frac{\rho_{mass,He}}{M_{He}}} - 1\right)^{-1} \tag{8}$$

4 Yield Spectra and Fitting Routine

In Eq. 8, the quantities Y_{prod} and Y_{dummy} are obtained from data; an example of the yield from a production and dummy run is shown in Fig. 4. The yield is binned in 1 MeV bins in ν, where $\nu = E - E'$, the difference between the incident and scattered electron energy. For this energy setting, the region of interest is from $\nu = 0$ to $\nu = 13$ MeV. For an ammonia run, this region includes the nitrogen and helium elastic peaks, which cannot be resolved individually, and a small percentage of "contamination" from the second peak. For a dummy run, this region includes the elastic peak and the "contamination" from the helium quasi-elastic peak. Since only elastic events are of interest, it is necessary to quantify the level of "contamination" from the second peak in the production and dummy yield spectra.

To fit the entire spectra, the fit is broken into two parts; the first and second peaks. The components of the fit differ between the dummy and production run, as described below.

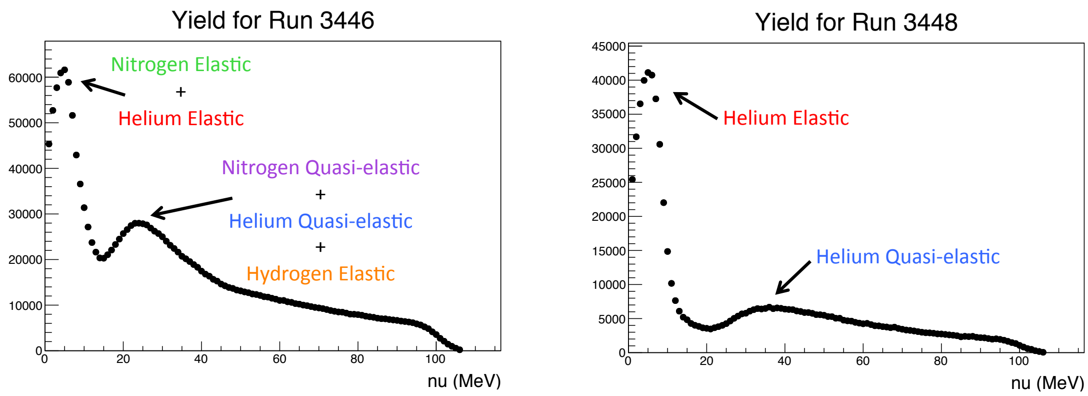

Figure 4: Yield spectra for a production run (left) and a dummy run (right).

4.1 Dummy Run

The yield spectrum for a dummy run is comprised predominately of one material, helium. In reality, this data also contains contributions from the aluminum target cell cap, but the contribution from Al is negligible. For this case, there are only two features to fit, the elastic peak and quasi-elastic peak. The elastic peak is not a true Gaussian, as it has some radiative tail, so a Landau-Gaussian convolution function is used to fit this peak. As it is only necessary to fit the left side of the quasi-elastic peak, a simple Gaussian function can be used. An example of this fit can be seen in Fig. 5; the level of contamination is generally small, less than 5% of the total area of the elastic peak.

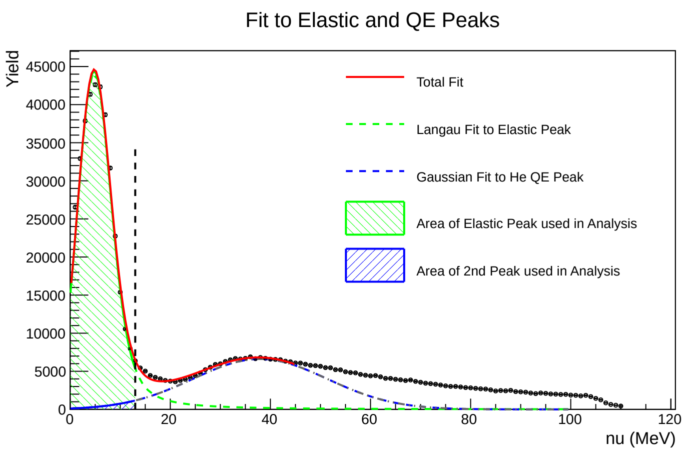

Figure 5: Dummy run 3448 with fit. The vertical dotted line represents the cut-off point for the region of interest for this analysis.

.

4.2 Ammonia Run

The yield spectrum for a production run is more complicated, as it has contributions from ammonia (nitrogen and hydrogen) and helium. The fit is, therefore, also more complicated. The elastic peak, which contains contributions from both nitrogen and helium elastic events, is again fit with a Landau-Gaussian (Langau) convolution fit. The second peak is comprised of nitrogen and helium quasi-elastic events as well as hydrogen elastic events. This peak is fit with the sum of three functions; the nitrogen and helium peaks are each fit with a Gaussian, and the hydrogen peak is fit with a Landau function. To understand the relative contributions form each material, the Quasi-Free Scattering (QFS) model was used within the g2psim package, a Monte Carlo simulation package based on Geant4.

4.2.1 Quasi-Free Scattering Model

The QFS model, developed by Lightbody and O'Connell [1] is used to predict cross sections for electron scattering. The cross section is accurate to within 20% for an incident electron energy between 0.5-5 GeV. The Fortran code parameterizes electron scattering using five reaction channels in the impulse approximation.

- Quasielastic scattering
- Two nucleon emission in the dip region
- Δ resonance production
- Higher nucleon resonance electroproduction (two resonances, centered at W = 1500 MeV and 1700 MeV)
- Deep Inelastic Scattering

This model will be used to understand the relative contributions from nitrogen, helium and hydrogen in the quasi-elastic region for an ammonia production run.

4.2.2 Matching QFS Model Parameters to Data

Within the model, there are three parameters that can be adjusted by the user:

- P_f: the Fermi momentum of the target nucleus
- Eps: the nucleon separation energy
- Epsd: the delta separation energy

For this analysis, the separation energies were chosen to best match the data, while the Fermi momentum values are reasonable for that material. The delta separation parameter does not contribute to this study, so it will not be discussed here.

Before fitting the production run, the data can be compared to the QFS model predictions to parameterize the different contributions. The dummy run is the simplest scenario to start with. Fig. 6 shows the simulation result compared to the data, with the associated QFS parameters. Similarly, the carbon dilution run can be used to understand the QFS parameters for carbon, which in turn can be used to estimate the Nitrogen parameters. The comparison between the QFS prediction and data for a carbon run is shown in Fig. 7. From these results it is possible to constrain the fit of the helium and nitrogen contributions to the overall fit. The hydrogen elastic peak contribution can be predicted using elastic from factors, which allows for additional constraints on the location and width of the hydrogen elastic peak.

In the overall fit to the second peak, the nitrogen and helium contributions are fit with a Gaussian function. The remaining hydrogen elastic peak is fit with a Landau function. An example of the total fit is seen in Fig. 8. The fits shown in Figs. 5 and 8 give the level of contamination from the second peak to the elastic peak, which is $\sim$5.7% for this example.

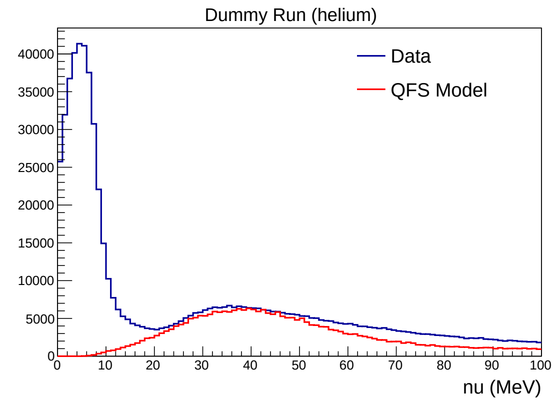

Figure 6: Dummy run compared to simulation output using QFS model.

.

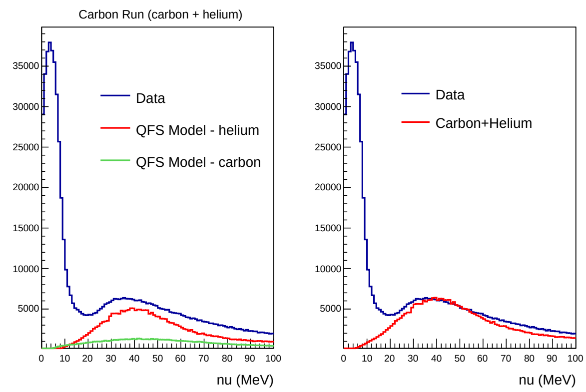

Figure 7: Dummy run compared to simulation output using QFS model.

.

4.3 Cross Section Model Input

The final piece of input required to extract the packing fraction is the cross section ratios σ_N/σ_{He} and σ_H/σ_{He}. The cross sections are determined using elastic form factors ([2],[3]). Since the cross section ratios are being combined with data, which already include radiative effects, it is necessary to first radiate the cross sections. This is accomplished using the g2psim package, which has been constructed to mirror the experimental conditions. An example of the simulation results is shown in Fig. 9. The cross section ratios were determined for each run individually, using the beam position values for that run.

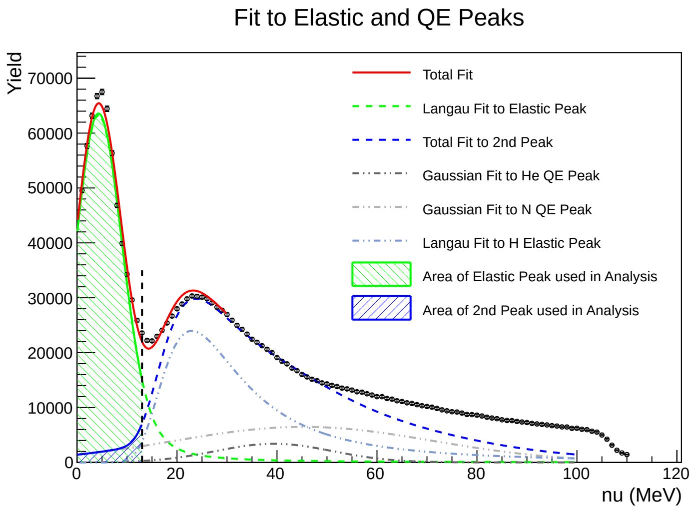

Figure 8: Production run 3446 with fit. The vertical dotted line represents the cut-off point for the region of interest for this analysis.

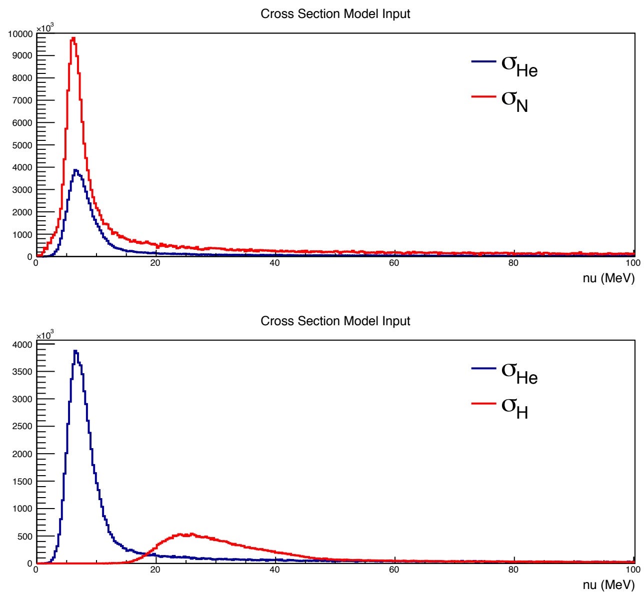

Figure 9: Elastic cross section results from g2psim for the 2.2 GeV, 2.5T, transverse setting.

5 Variation in Yields

For several settings, there was a significant variation seen in the yields for different runs taken at the elastic setting. In an effort to flush out the cause for this variation, many parameters were checked to test the effect on the yield for each run. These checks will be described for each configuration in this section.

5.1 E_{beam} = 2.2 GeV, B_{target} =2.5 T, Transverse (setting 1)

The normalized yields (calculated using Eq. 1) are shown in Fig. 10, split into the two materials used for this setting. The normalization constants for each run are detailed in Table 1. For this setting, the yields vary significantly; there is variation seen in the amplitude of the elastic peak, as well as a shift in ν.

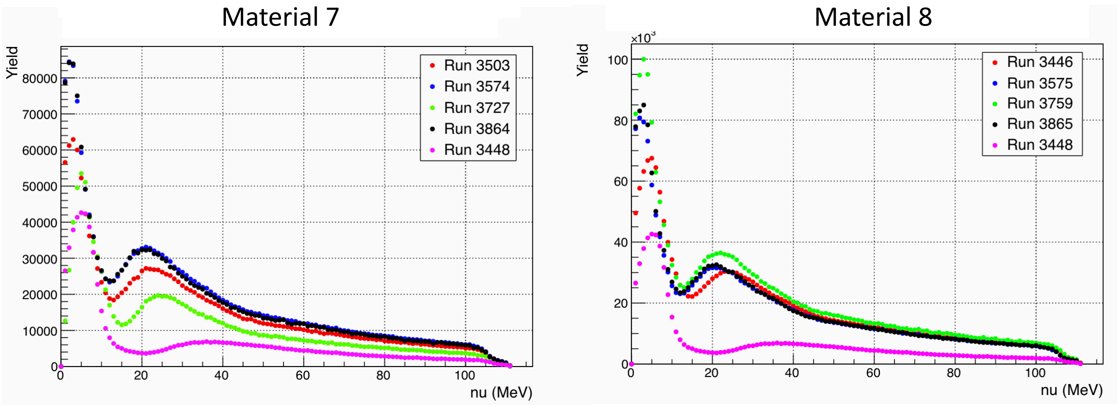

Figure 10: Yields for elastic runs in setting 1 (materials 7 and 8).

Table 1: E_{beam} = 2.2 GeV, 2.5T 90 deg Target Field, p0 = 2.228 GeV/c								
Run #	Material	Charge (μC)	Livetime	CerDetEff	PRDetEff	MultiTrackEff	TriggerEff	Prescale
3446	8	66.583	0.8945	0.999963	0.999795	0.91625	0.999843	15
3503	7	14.5084	0.91517	0.999948	0.999835	0.919614	0.999838	15
3574	7	18.9126	0.943908	0.999973	0.999876	0.904337	0.999852	20
3575	8	17.9473	0.94949	0.949493	0.99995	0.907999	0.999856	20
3727	7	16.594	0.94114	0.941136	0.999945	0.91471	0.999857	18
3759	8	11.3651	0.92468	0.92468	0.999927	0.90849	0.999867	19
3864	7	8.91995	0.85727	0.999947	0.999799	0.90532	0.999858	20
3865	8	9.64021	0.944305	0.944305	0.999905	0.90737	0.999861	20
3448	dummy	8.63567	0.947817	0.999947	0.999858	0.966655	0.999835	7

Table 1

The ratio of the raw singles trigger rate (T3 on the LHRS) divided by the beam current for each run is shown in Fig. 11. For the same kinematic settings, this ratio should be stable; for this setting variation is seen in this quantity. The likely reason for this discrepancy is that the raster size was changed following a Moller measurement on March 30^{th}. After the measurement, higher rates were seen in the third arm detector, suggesting that the beam was scraping something. Reducing the raster size from 2 cm to 1.8 cm caused the rates to return to normal. For this set of runs, the change in raster size occurred after run 3503, but before run 3574. The change is raster size can be seen in Fig. 12. It is also apparent from these plots that the beam position was also shifting throughout this series of runs. The central beam position with uncertainty for each run is plotted in Fig. 13.

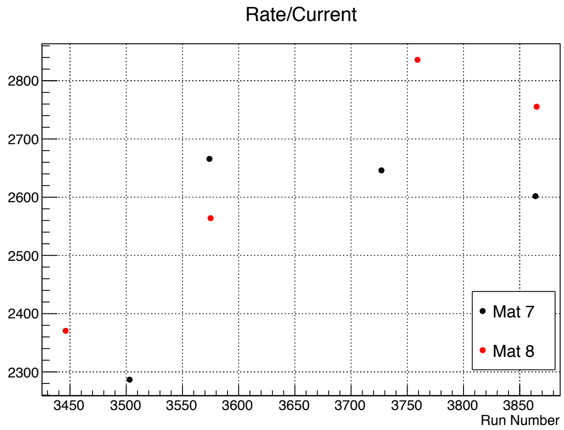

Figure 11: The ratio of T3 rate to current for setting 1.

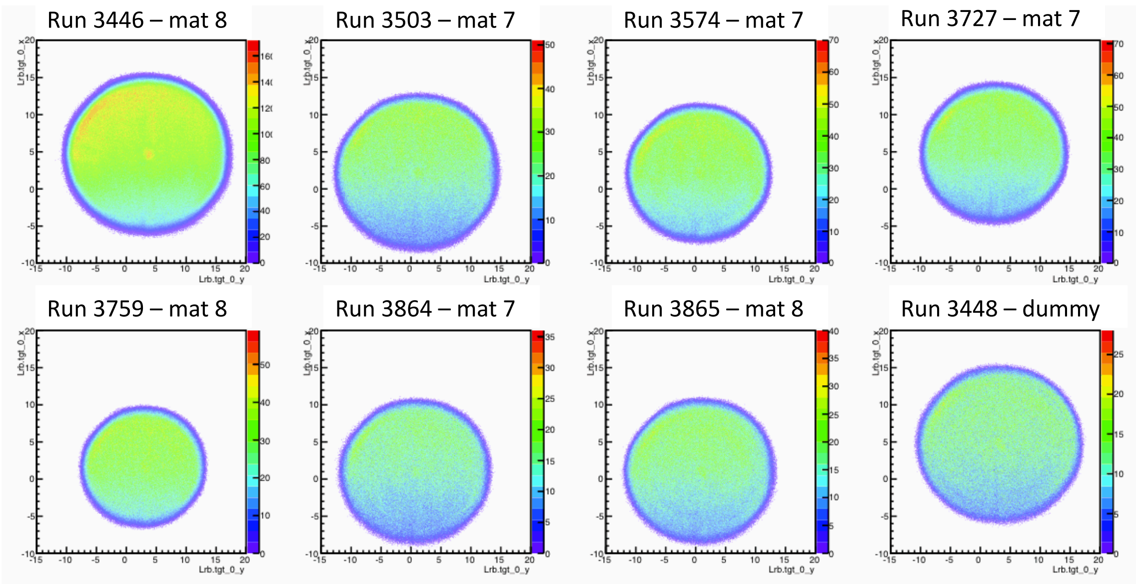

Figure 12: Raster patterns for setting 1 (target x vs target y).

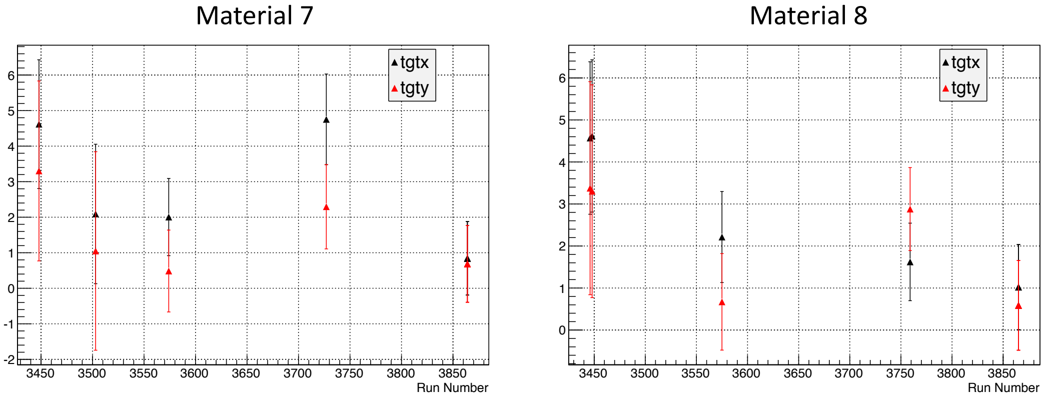

Figure 13: Beam position at the target for elastic runs in setting 1. The y-axis shows the x/y beam position in mm.

Since the only dummy run in this setting was taken with the large raster, it may not be appropriate to compare the yield to production runs taken with the smaller raster size without first applying a beam size correction to account for this difference.

5.2 E_{beam} = 1.7 GeV, B_{target} =2.5 T, Transverse (setting 2)

The normalized yields and associated normalization constants are shown in Fig. 14 and Table 2. The yields are considerably more stable for this set of runs, but there does appear to be some drifting.

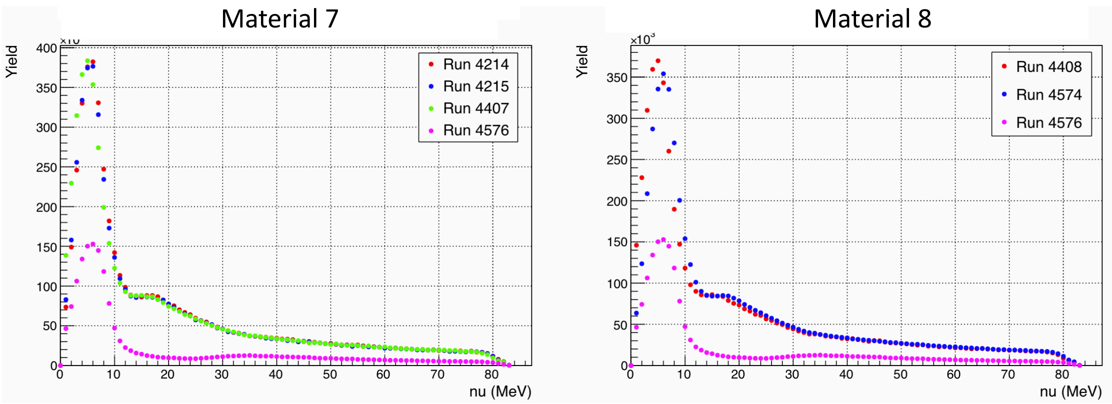

Figure 14: Yields for elastic runs in setting 1 (materials 7 and 8).

.

Table 2: E_{beam} = 1.7 GeV, 2.5T 90 deg Target Field, p0 = 1.691 GeV/c

Run #	Material	Charge (μC)	Livetime	CerDetEff	PRDetEff	MultiTrackEff	TriggerEff	Prescale
4214	7	7.45578	0.950733	0.999943	0.999755	0.819318	0.999815	44
4215	7	6.92801	0.934386	0.999908	0.99976	0.82563	0.99983	40
4407	7	5.95016	0.830349	0.999906	0.99979	0.817849	0.999804	30
4408	8	5.95857	0.844765	0.999951	0.9998	0.822028	0.999801	30
4574	8	45.1338	0.874485	0.999906	0.999794	0.817768	0.999808	34
4576	dummy	6.61051	0.870051	0.999928	0.999873	0.936884	0.999777	11

Table 2

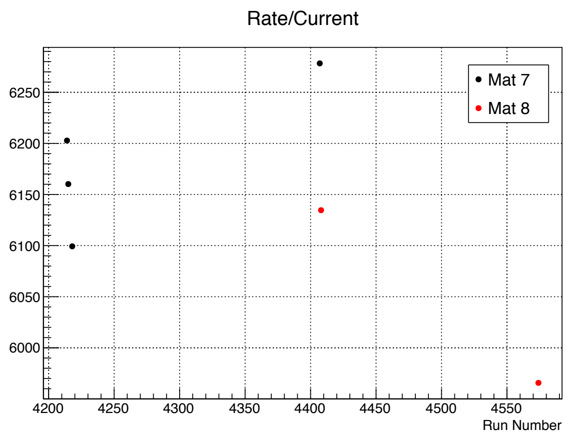

Figure 15: The ratio of T3 rate to current for setting 2.

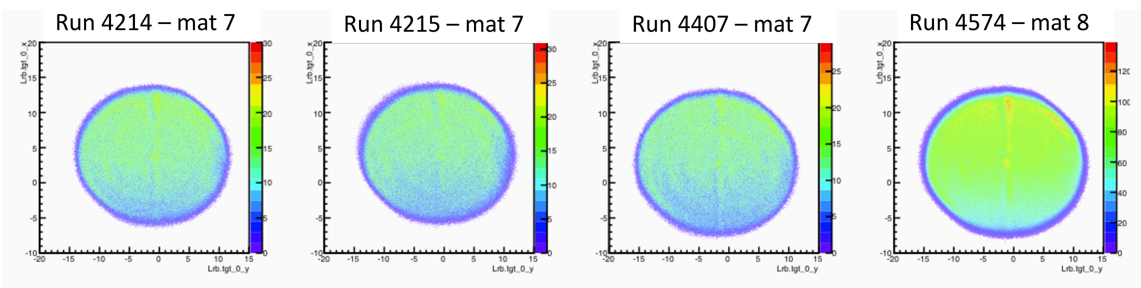

Figure 16: Raster patterns for setting 2 (target x vs target y).

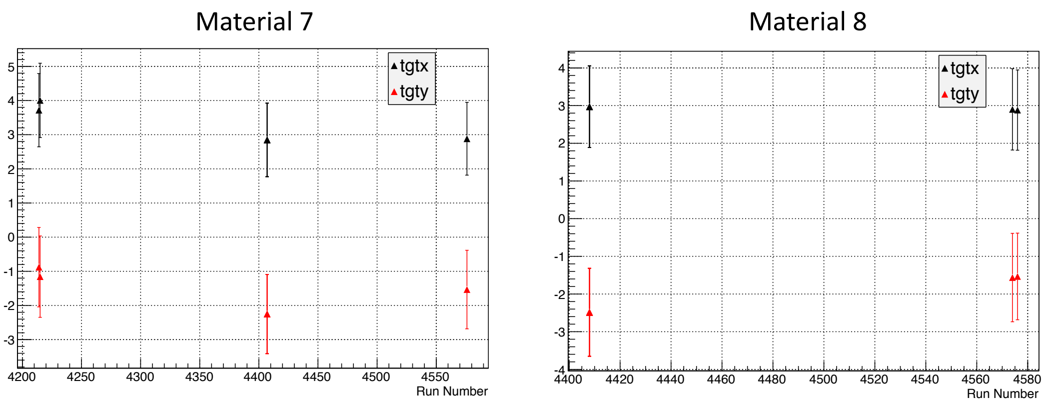

Figure 17: Beam position at the target for elastic runs in setting 2. The y-axis shows the x/y beam position in mm.

5.3 E_{beam} = 1.1 GeV, B_{target} = 2.5 T, Transverse (setting 3)

The normalized yields and associated normalization constants are shown in Fig. 18 and Table 3. Runs were also taken in this setting with a short ammonia cell (material 14), which was 1.295 cm in length. For some runs, beam position information was not available due to the low current limitations of the BPMs. In these cases, neighboring runs were included in the raster and beam position plots shown below (Fig. 20 and 21).

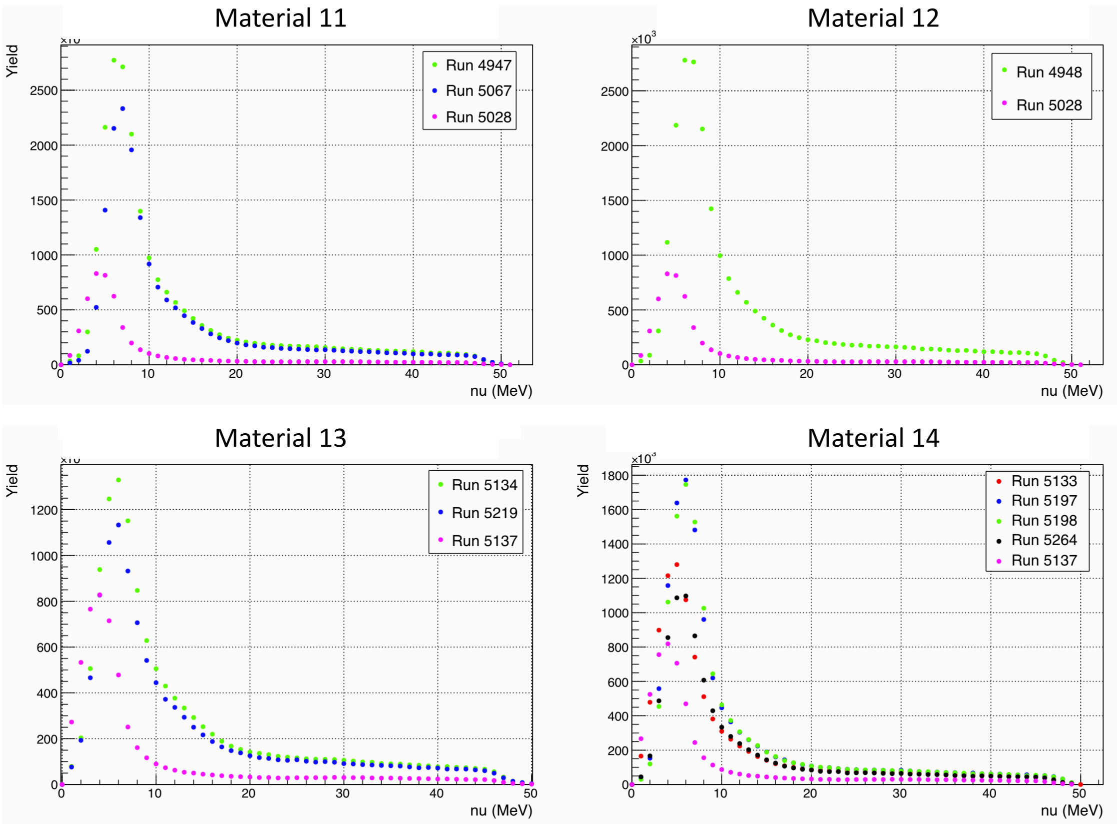

Figure 18: Yields for elastic runs in setting 2 (materials 11, 12, 13 and 14). Material 14 is a short cell.

.

Table 3: E_{beam} = 1.2 GeV, 2.5T 90 deg Target Field, p0 = 1.151 GeV/c								
Run #	Material	Charge (μC)	Livetime	CerDetEff	PRDetEff	MultiTrackEff	TriggerEff	Prescale
4947	11	1.5631	0.925943	0.999757	0.999535	0.849666	0.999761	34
4948	12	2.00492	0.921853	0.999741	0.999568	0.847924	0.999747	34
5067	11	3.66682	0.92828	0.999554	0.999361	0.736755	0.999732	65
5133	14	21.3065	0.982791	0.998961	0.998451	0.609576	0.999675	150
5134	13	18.2617	0.91747	0.997098	0.997708	0.49526	0.999599	150
5197	14	3.27598	0.89407	0.999723	0.999387	0.793361	0.999715	45
5198	14	3.36181	0.889436	0.999725	0.999452	0.791059	0.999708	45
5219	13	8.08825	0.880206	0.996388	0.998062	0.484659	0.99959	137
5264	14	9.05938	0.922331	0.998806	0.998848	0.594396	0.99965	109
5028	dummy	7.30217	0.885043	0.999836	0.999423	0.812038	0.999655	40
5137	dummy	14.3847	0.921307	0.999247	0.998813	0.822588	0.999676	100

Table 3

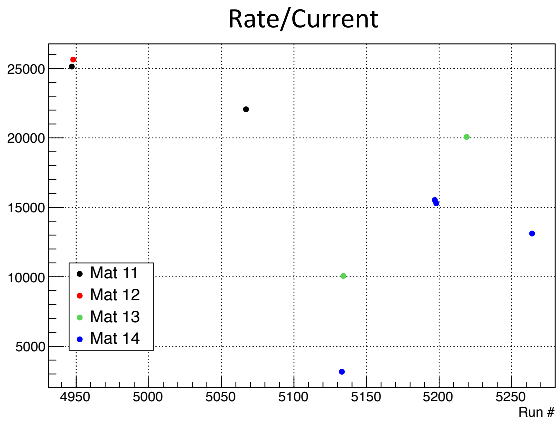

Figure 19: The ratio of T3 rate to current for setting 3.

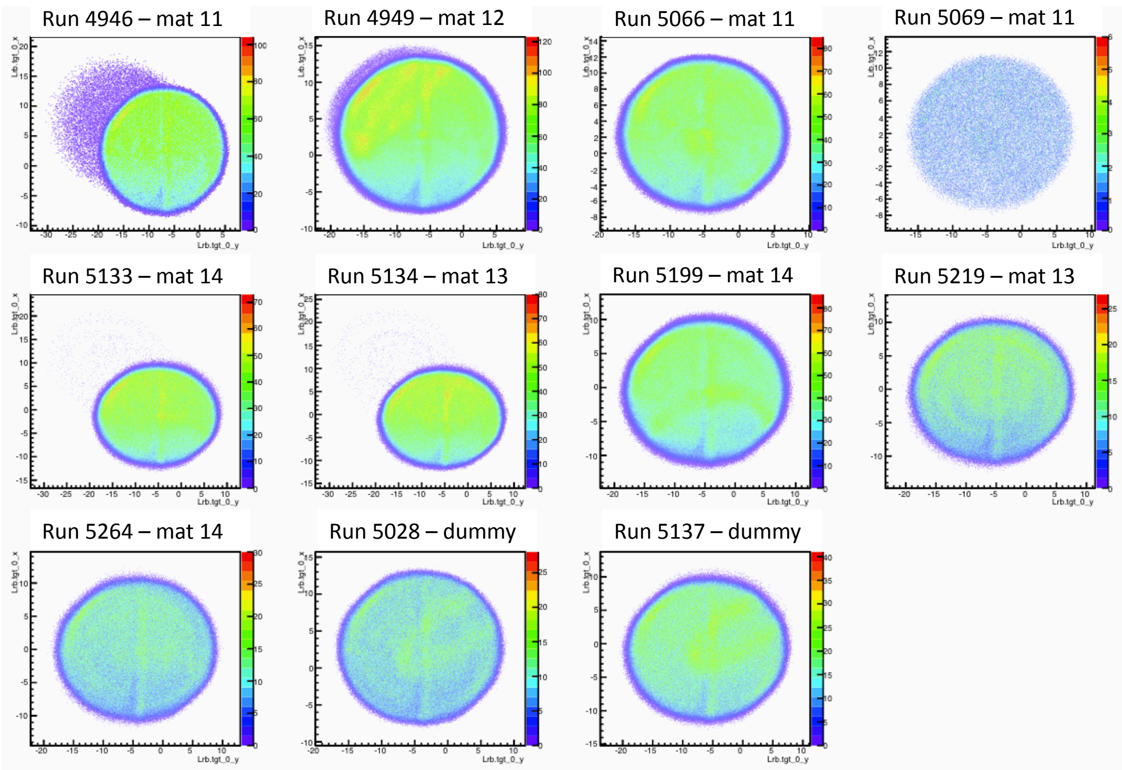

Figure 20: Raster patterns for setting 3 (target x vs target y).

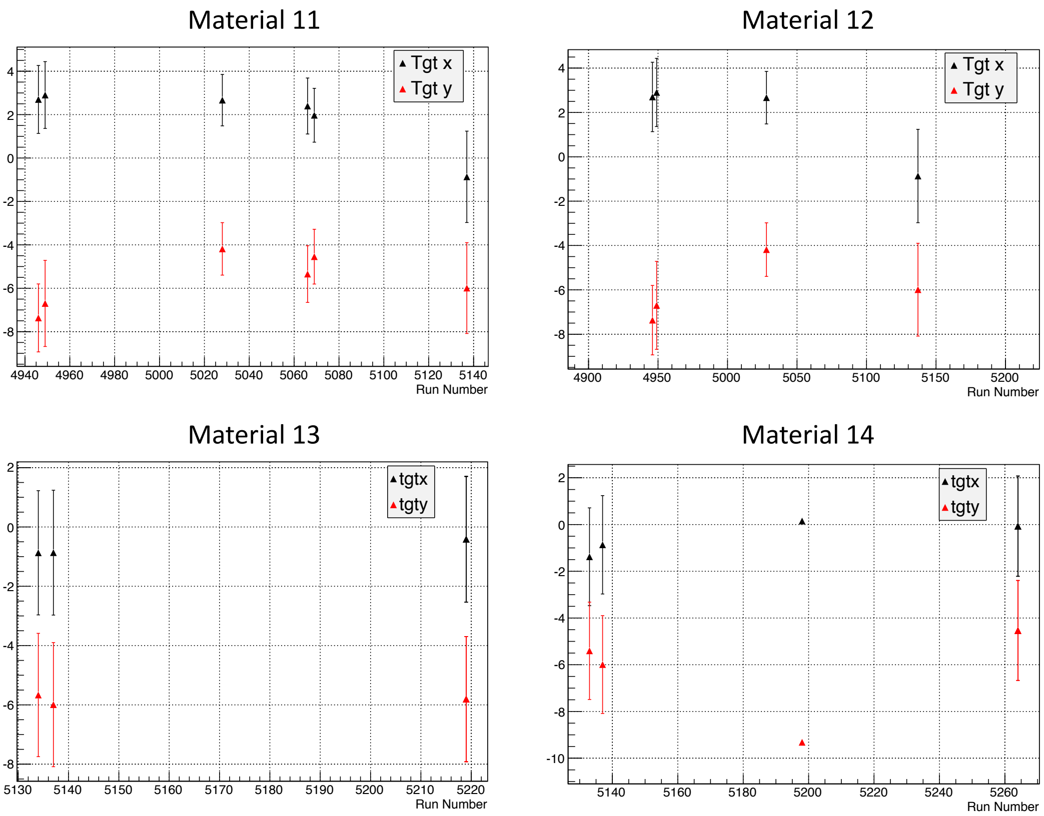

Figure 21: Beam position at the target for elastic runs in setting 3. The y-axis shows the x/y beam position in mm. If no error bars are shown, than no error was available for that data point.

.

5.4 E_{beam} = 2.2 GeV, B_{target} =5 T, Longitudinal (setting 4)

The normalized yields and associated normalization constants are shown in Fig. 22 and Table 4. There is some drifting seen in the yields for this set of runs.

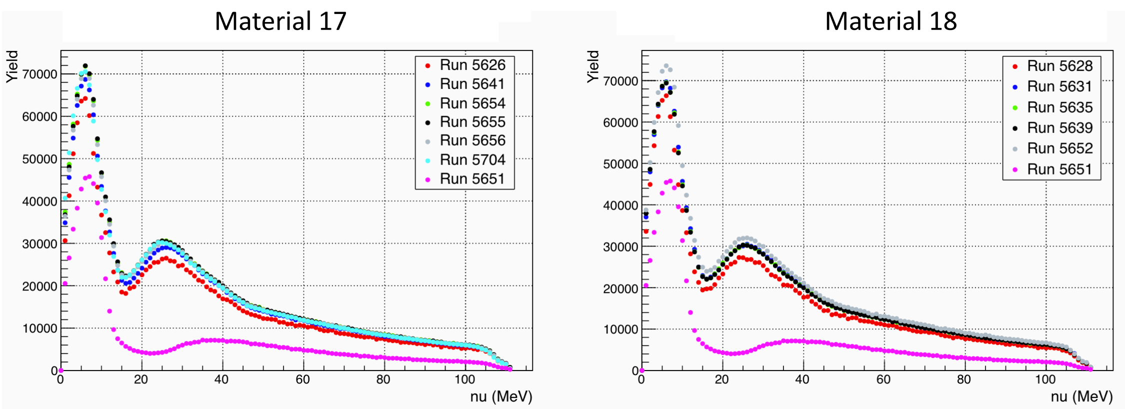

Figure 22: Yields for elastic runs in setting 4 (materials 17 and 18).

.

Table 4: E_{beam} = 2.2 GeV, 5T 0 deg Target Field, p0 = 2.228 GeV/c								
Run #	Material	Charge (μC)	Livetime	CerDetEff	PRDetEff	MultiTrackEff	TriggerEff	Prescale
5626	17	6.94362	0.911514	0.999914	0.999865	0.919026	0.999766	15
5628	18	7.22268	0.874545	0.999891	0.999850	0.916626	0.999769	14
5631	18	33.5003	0.878033	0.999930	0.999860	0.916148	0.999774	14
5635	18	44.1951	0.884286	0.999931	0.999863	0.917281	0.999760	14
5639	18	44.8087	0.876390	0.999937	0.999861	0.914603	0.999758	14
5641	17	47.4714	0.866277	0.999918	0.999867	0.912310	0.999766	14
5652	18	29.8818	0.898077	0.999925	0.999766	0.911289	0.999770	16
5654	17	48.7824	0.920883	0.999928	0.999859	0.915638	0.999767	16
5655	17	35.7286	0.926231	0.999942	0.999853	0.917658	0.999769	16
5656	17	48.04	0.937350	0.999930	0.999869	0.917694	0.999763	16
5704	17	42.8975	0.852226	0.999940	0.999880	0.914939	0.999762	13
5651	dummy	7.53653	0.916283	0.999982	0.999890	0.962627	0.999650	7

Table 4

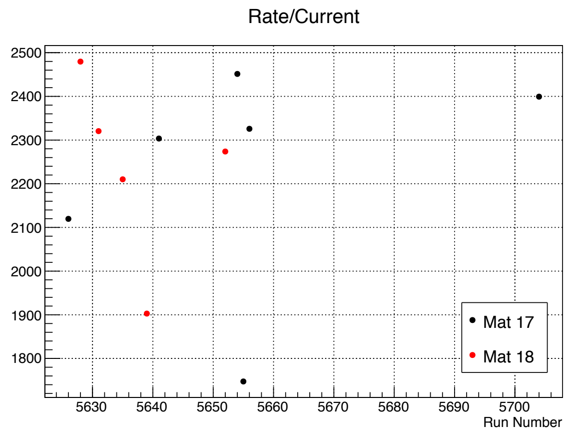

Figure 23: The ratio of T3 rate to current for setting 4.

.

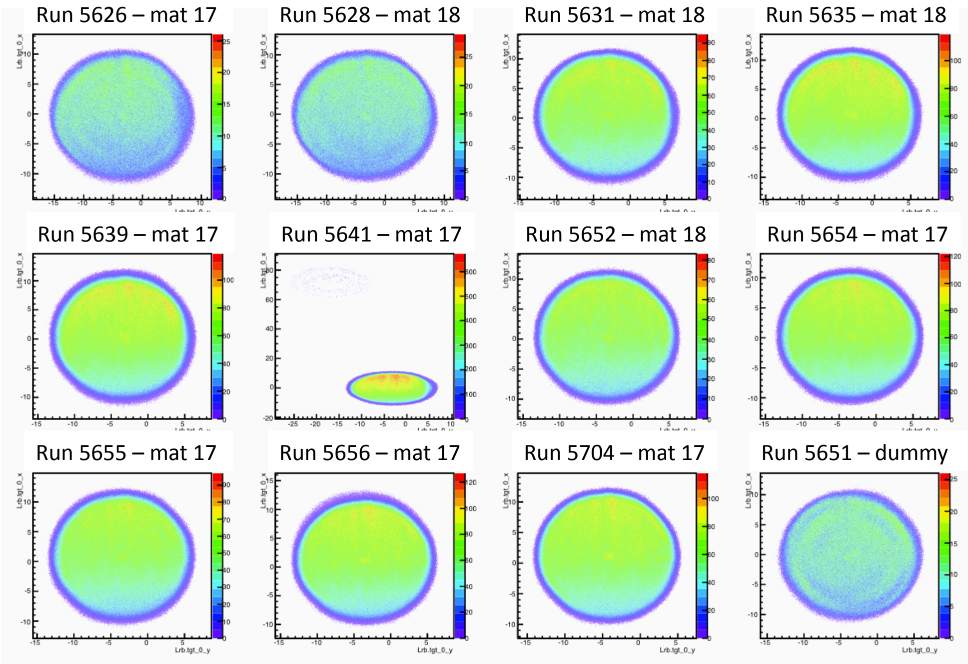

Figure 24: Raster patterns for setting 4 (target x vs target y).

.

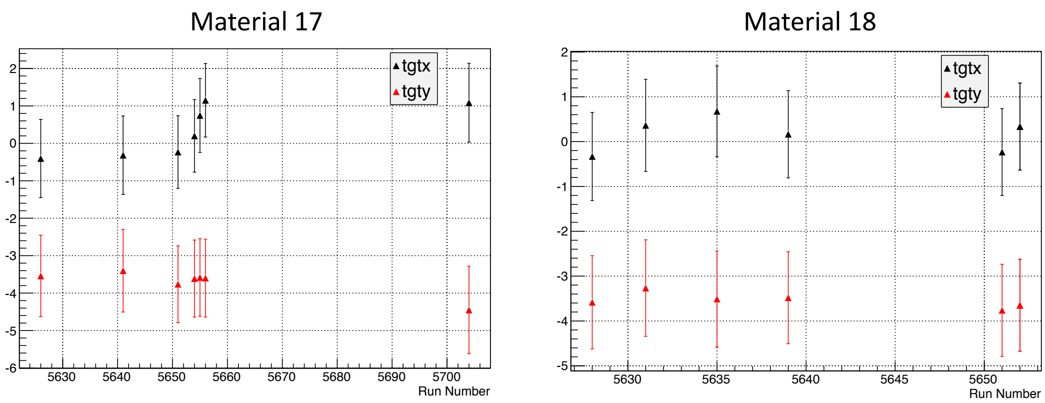

Figure 25: Beam position at the target for elastic runs in setting 4. The y-axis shows the x/y beam position in mm.

5.5 E_{beam} = 2.2 GeV, B_{target} =5 T, Transverse (setting 5)

The normalized yields and associated normalization constants are shown in Fig. 26 and Table 5. There is some drifting seen in the yields for this set of runs.

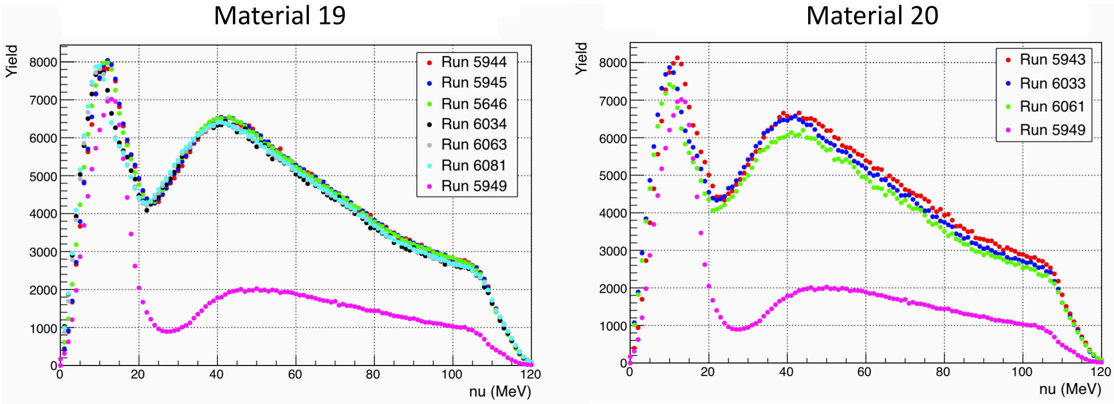

Figure 26: Yields for elastic runs in setting 5 (materials 19 and 20).

.

Table 5: E_{beam} = 2.2 GeV, 5T 90 deg Target Field, p0 = 2.228 GeV/c								
Run #	Material	Charge (μC)	Livetime	CerDetEff	PRDetEff	MultiTrackEff	TriggerEff	Prescale
5943	20	7.86738	0.906548999	0.999927	0.999883	0.9765222	0.999799	4
5944	19	14.6027	0.905672997	0.99995	0.99987	0.976511094	0.999794	4
5945	19	31.6538	0.900568001	0.999947	0.99986	0.975952756	0.999802	4
5946	19	50.4904	0.916153997	0.999946	0.999872	0.977117658	0.999798	4
6033	20	13.5855	0.933069997	0.999916	0.999881	0.97287032	0.999807	5
6034	19	13.4473	0.934446	0.999926	0.999863	0.973591831	0.999798	5
6061	20	9.80441	0.908611998	0.999933	0.999899	NULL	0.999804	5
6063	19	38.1677	0.878386997	0.999942	0.999876	0.968488247	0.999796	5
6081	19	65.8659	0.884966001	0.99994	0.999877	0.969076186	0.999796	5
5949	dummy	13.0383	0.904019997	0.999938	0.999898	0.988858981	0.999816	2

Table 5

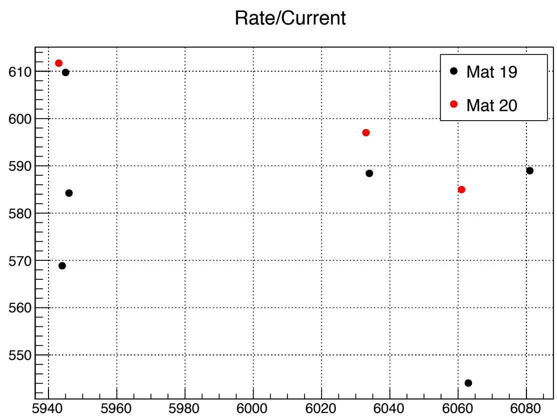

Figure 27: The ratio of T3 rate to current for setting 5.

.

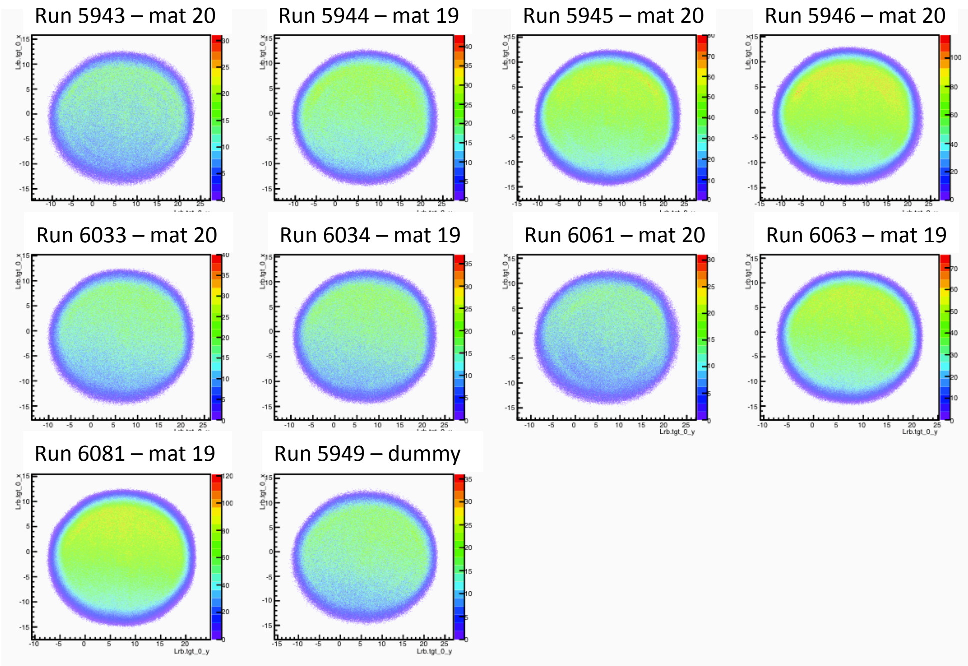

Figure 28: Raster patterns for setting 5 (target x vs target y). The events in the upper left corner of the plot for run 5641 suggest the beam position was slightly unstable for this run.

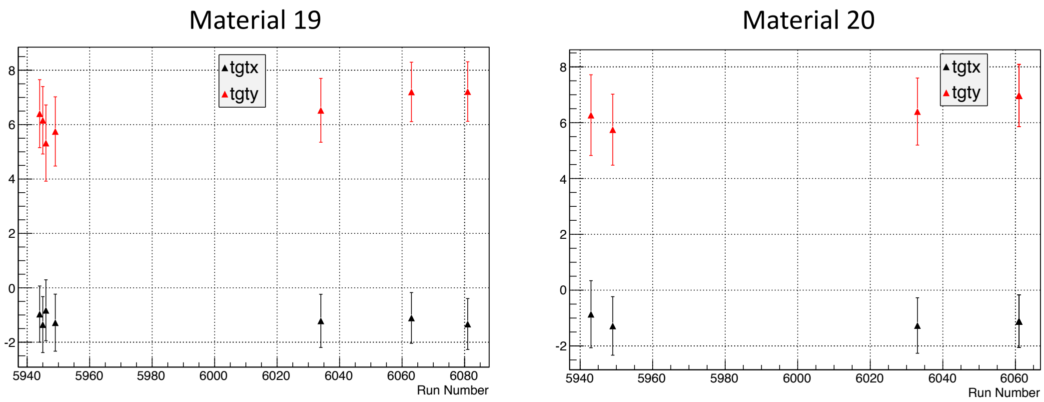

Figure 29: Beam position at the target for elastic runs in setting 5. The y-axis shows the x/y beam position in mm.

6 Uncertainty

There are several contributions to the overall uncertainty for the packing fraction. Setting 1 (runs 3448 and 3446) will be used as an example.

- Standard propagation of uncertainty; the contributing factors are listed in Table 6. The uncertainty of σ_N and σ_{He} was determined to be 3% and the uncertainty of σ_H was determined to be 1%.
- To calculate the packing fraction, the quantity Y_{prod} and Y_{dummy} are determined by summing over the elastic peak, while the level of contamination is determined using the fitting routine described

above. $Y_{prod} = Y_{elastic} - Y_{contam} + Y_H$, where $Y_{elastic}$ is the sum over the elastic peak, Y_{contam} is the contamination determined from the fit, and Y_H is the hydrogen contribution, which is also determined from the fit. $Y_{dummy} = Y'_{elastic} - Y'_{contam}$, where $Y'_{elastic}$ is the sum over the elastic peak of the dummy run, and Y'_{contam} is the contamination determined from the fit. The difference between the fit and sum is also included in the overall uncertainty, the area from the fit is calculated by adding the area of the elastic and contamination fits. (Table 7).

Table 6: Contributions to Uncertainty		
Quantity	Value	Uncertainty
l_{tg}	28.2 mm	0.1 mm
l_{tot}	37 mm	0.1 mm
Y_{prod}	618866.1	1534.8
Y_{dummy}	356016.1	641.2
σ_N/σ_{He}	2.9149	4.24%
σ_H/σ_{He}	0.0042	3.16%

Table 6

Table 7: Contributions to Uncertainty			
Run	Sum (ν = 0-13)	Area from Fit (ν = 0-13)	% Difference
Production	647701.9	636250.2	1.78
Dummy	362430.8	358233.7	1.16

Table 7

7 Results

A example of the fit to the dummy and production run is shown for each setting, followed by a table of the packing fraction results for each elastic run. The table also includes the quantity Y_{prod}/Y_{dummy}, which is the ratio of the sum over the elastic peak of the production and dummy runs, and the quantity σ_N/σ_{He}, which is the cross section (from model) ratio determined using the beam position for that run.

7.1 Setting 1

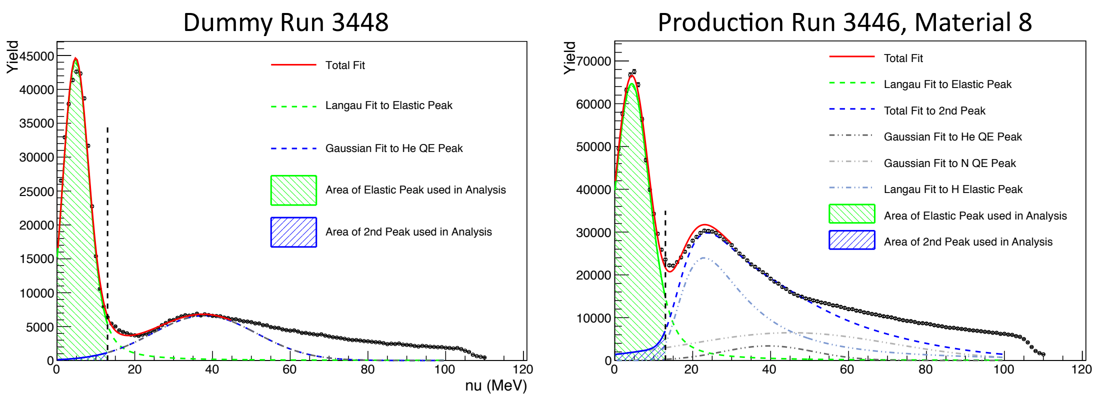

Figure 30: Fit examples for the 2.2 GeV, 2.5 T, Transverse setting (setting 1). The dummy run (3448) is on the left and the ammonia run (3446) is on the right.

Table 8: E_{beam} = 2.2 GeV, 2.5T 90 deg Target Field				
Run #	Material	Y_{prod}/Y_{dummy}	σ_N/σ_{He}	Packing Fraction ± Uncertainty
3446	8	1.787	2.201	0.505 ± 0.013
3503	7	1.464	1.860	0.327 ± 0.007
3574	7	1.821	1.833	0.648 ± 0.018
3575	8	1.780	1.884	0.606 ± 0.015
3727	7	1.188	2.212	0.074 ± 0.003
3759	8	2.180	1.929	0.894 ± 0.031
3864	7	1.830	1.652	0.795 ± 0.031
3865	8	1.854	1.661	0.810 ± 0.031

Table 8: Results for setting 1.

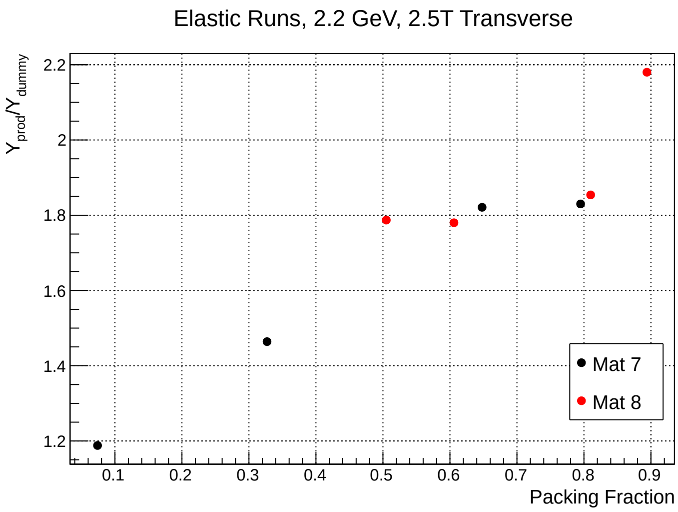

Figure 31: Relation between the packing fraction and the ratio of the production yield over the dummy yield.

7.2 Setting 2

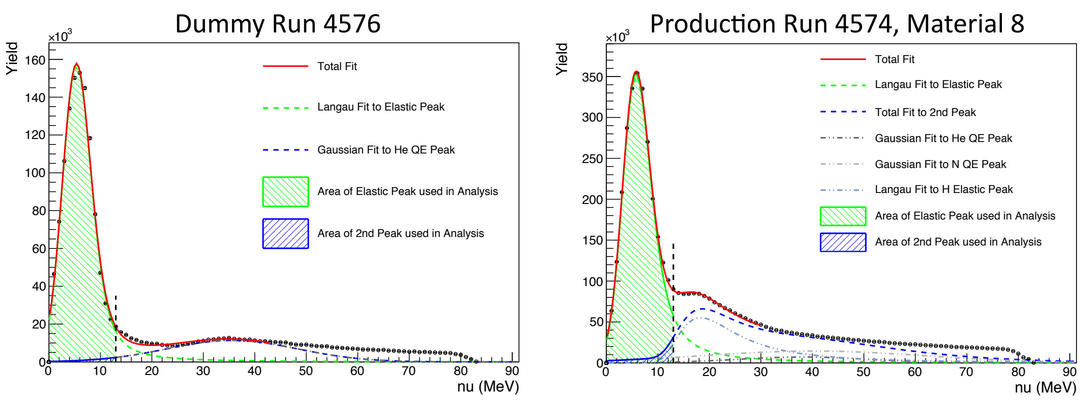

Figure 32: Fit examples for the 1.7 GeV, 2.5 T, Transverse setting (setting 2). The dummy run (4576) is on the left and the ammonia run (4574) is on the right.

Table 9: E_{beam} = 1.7 GeV, 2.5T 90 deg Target Field				
Run #	Material	Y_{prod}/Y_{dummy}	σ_N/σ_{He}	Packing Fraction ± Uncertainty
4214	7	2.497	3.829	0.467 ± 0.012
4215	7	2.472	3.822	0.460 ± 0.010
4407	7	2.551	3.705	0.503 ± 0.007
4408	8	2.482	3.677	0.484 ± 0.007
4574	8	2.395	3.732	0.452 ± 0.015

Table 9: Results for setting 2.

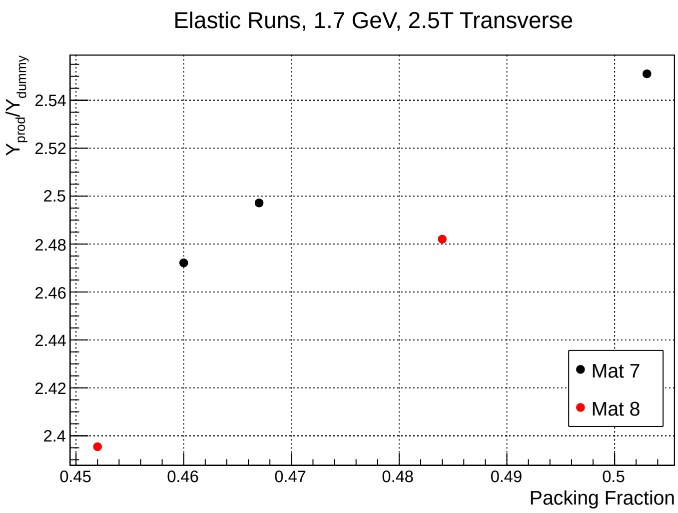

Figure 33: Relation between the packing fraction and the ratio of the production yield over the dummy yield.

7.3 Setting 3

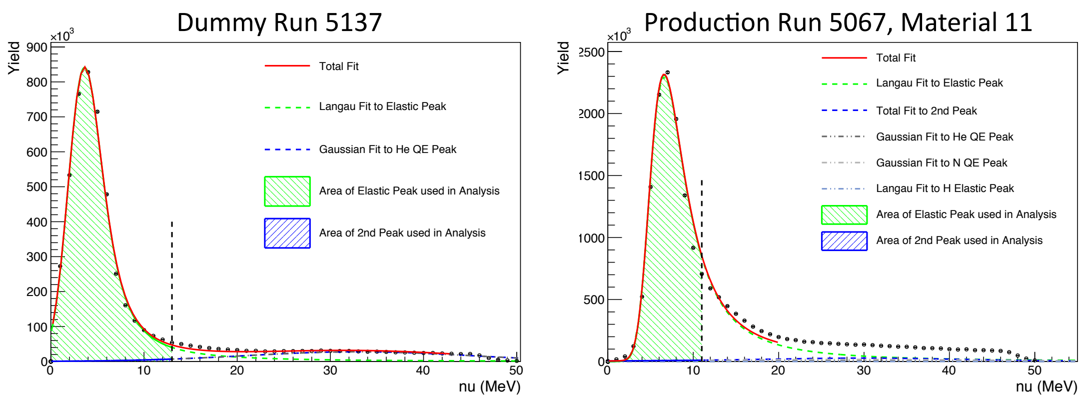

Figure 34: Fit examples for the 1.1 GeV, 2.5 T, Transverse setting. The dummy run (5137) is on the left and the ammonia run (5067) is on the right.

Table 10: E_{beam} = 1.1 GeV, 2.5T 90 deg Target Field				
Run #	Material	Y_{prod}/Y_{dummy}	σ_N/σ_{He}	Packing Fraction ± Uncertainty
4947	11	3.585	6.235	0.444 ± 0.029
4948	12	3.651	6.235	0.456 ± 0.030
5067	11	2.937	5.994	0.350 ± 0.012
5134	13	1.896	5.774	0.171 ± 0.011
5219	13	1.630	5.937	0.116 ± 0.006

Table 10: Results for setting 3.

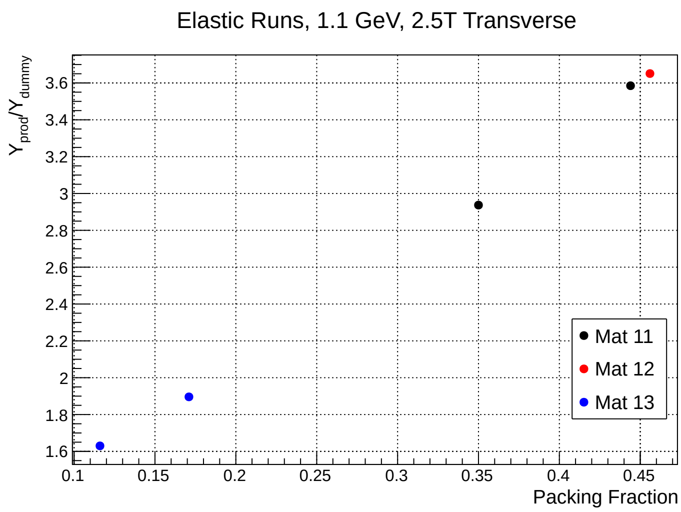

Figure 35: Relation between the packing fraction and the ratio of the production yield over the dummy yield.

Table 11: E_{beam} = 1.1 GeV, 2.5T 90 deg Target Field (short cell)				
Run #	Material	Y_{prod}/Y_{dummy}	σ_N/σ_{He}	Packing Fraction ± Uncertainty
5133	14	1.735	7.076	0.229 ± 0.0086
5197	14	2.184	7.499	0.347 ± 0.0153
5198	14	2.143	7.499	0.335 ± 0.0155
5264	14	1.493	7.440	0.143 ± 0.0073

Table 11: Results for setting 3 (short cell).

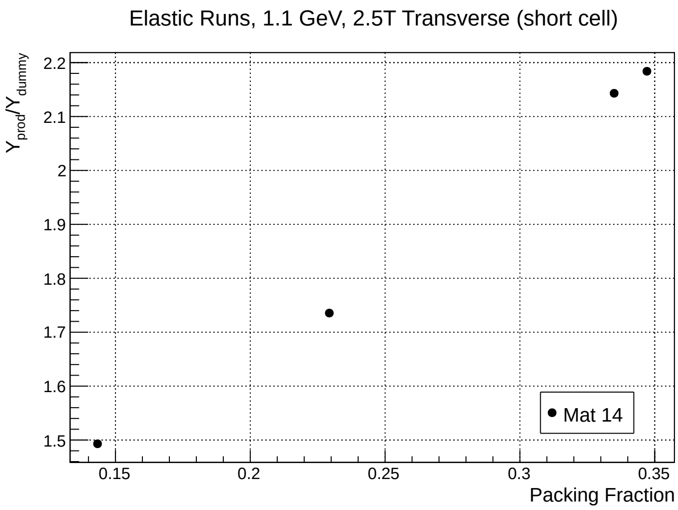

Figure 36: Relation between the packing fraction and the ratio of the production yield over the dummy yield.

7.4 Setting 4

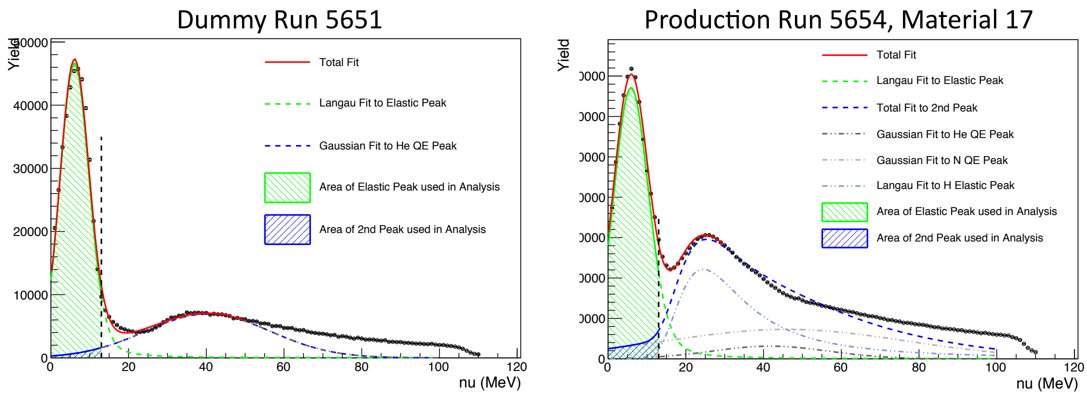

Figure 37: Fit examples for the 2.2 GeV, 5 T, Longitudinal setting. The dummy run (5651) is on the left and the ammonia run (5654) is on the right.

Table 12: E_{beam} = 2.2 GeV, 5T 0 deg Target Field				
Run #	Material	Y_{prod}/Y_{dummy}	σ_N/σ_{He}	Packing Fraction ± Uncertainty
5626	17	1.439	1.772	0.366 ± 0.015
5628	18	1.499	1.773	0.446 ± 0.018
5631	18	1.670	1.936	0.531 ± 0.022
5635	18	1.663	1.937	0.525 ± 0.021
5639	18	1.660	1.886	0.546 ± 0.023
5641	17	1.607	1.810	0.515 ± 0.022
5652	18	1.782	1.898	0.619 ± 0.027
5654	17	1.702	1.859	0.579 ± 0.025
5655	17	1.704	1.942	0.537 ± 0.023
5656	17	1.672	1.974	0.492 ± 0.021
5704	17	1.660	1.841	0.551 ± 0.022

Table 12: Results for setting 4.

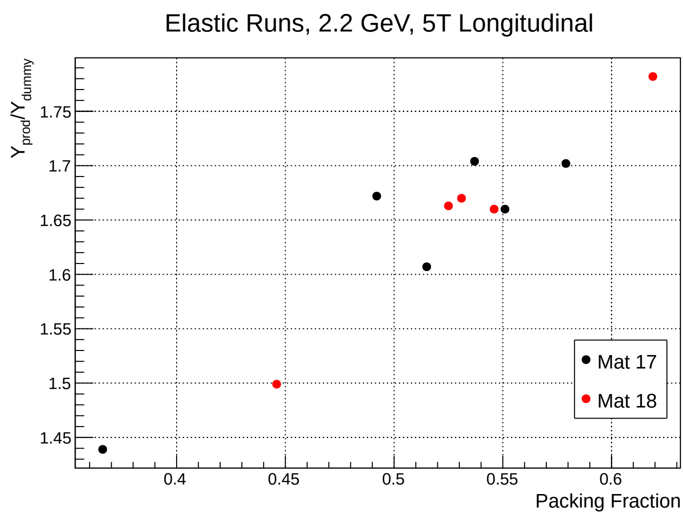

Figure 38: Relation between the packing fraction and the ratio of the production yield over the dummy yield.

7.5 Setting 5

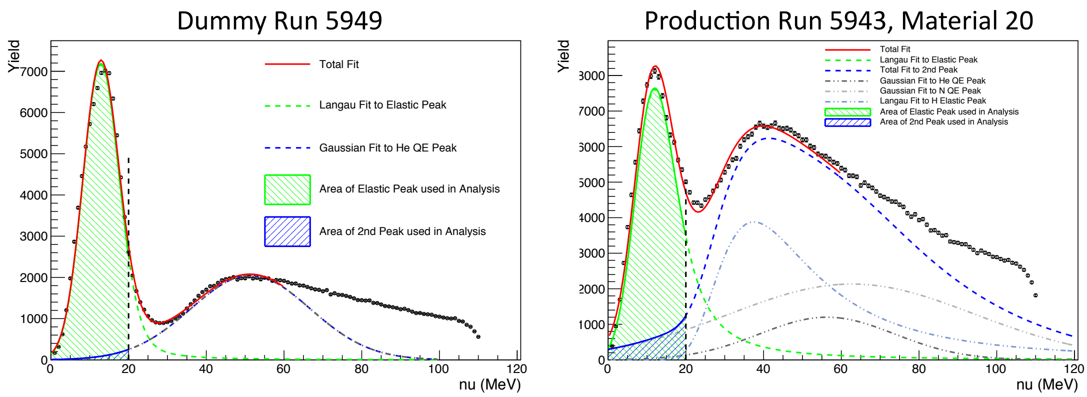

Figure 39: Fit examples for the 2.2 GeV, 5 T, Transverse setting. The dummy run (5949) is on the left and the ammonia run (5943) is on the right.

Table 13: E_{beam} = 2.2 GeV, 5T 90 deg Target Field				
Run #	Material	Y_{prod}/Y_{dummy}	σ_N/σ_{He}	Packing Fraction $\pm$ Uncertainty
5943	20	1.336	1.144	0.552 $\pm$ 0.052
5944	19	1.317	1.118	0.565 $\pm$ 0.056
5945	19	1.333	1.083	0.660 $\pm$ 0.072
5946	19	1.353	1.111	0.684 $\pm$ 0.074
6033	20	1.351	1.090	0.633 $\pm$ 0.064
6034	19	1.345	1.105	0.655 $\pm$ 0.071
6061	20	1.351	1.118	0.600 $\pm$ 0.049
6063	19	1.325	1.134	0.479 $\pm$ 0.040
6081	19	1.342	1.112	0.587 $\pm$ 0.055

Table 13: Results for setting 5.

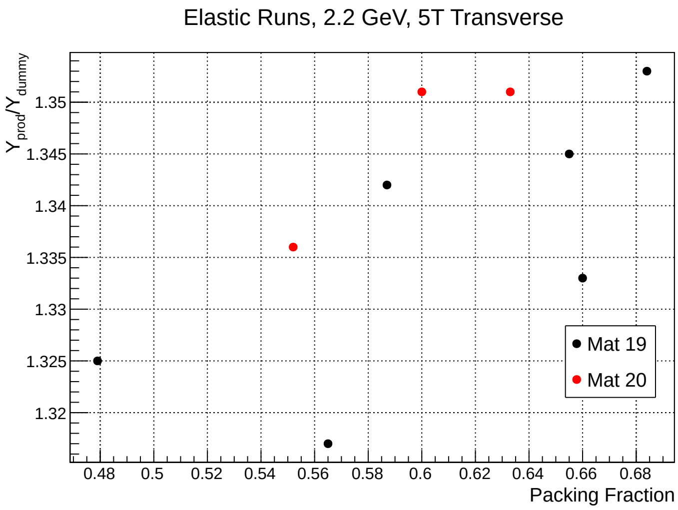

Figure 40: Relation between the packing fraction and the ratio of the production yield over the dummy yield.

8 Summary

The NH_3 target used in the g_2^p experiment is not a pure proton target; events that scatter from unpolarized target material will dilute the e-P scattering asymmetry. The dilution factor, which represents the ratio of the electron rate from the free, polarizable protons to the total rate from all nucleons in the material, will correct for this. In order to understand the dilution factor, the packing fraction, or the proportion of ammonia target material to the liquid helium in which it is immersed, must first be extracted.

The packing fraction was extracted for each of the 10 material samples used in the g_2^p experiment. Variation was seen in the elastic yields from run to run, which resulted in a variation in the packing fraction. It is unclear what is causing the variation in the yield for some settings, but a possibility is a drift in the beam position from run to run. A study is currently being done to understand the effect of the fluctuating beam position on the cross section and acceptance. Once this study is complete, the packing fraction values can be recalculated to include this correction.

References

[1] J.W. Lightbody Jr, J.S. O'Connell, Computers in Physics **2**, 57 (1988)

[2] S. Venkat et al, Phys. Rev. C, **83** (2011) 015203

[3] K. De Jager et al, At. Data Nucl. Data Tables, **14** (1974)

[4] R. Zielinski, *Determining the Trigger Efficiency for E08-027*, E08-027 Technical Note (2012)

[5] M. Cummings, *Efficiency Studies and PID Cut Optimization*, E08-027 Technical Note (2013)

[6] J. Liu, *VDC Multi-Track Efficiency Study*, E08-027 Technical Note (2015)